ACTA ACUSTICA UNITED WITH ACUSTICA
Vol. 96 (2010) 82 – 91

DOI 10.3813/AAA.918259

Sound Reflections from Concave Spherical Surfaces. Part I: Wave Field Approximation

Martijn Vercammen
Peutz bv, Lindenlaan 41, PO Box 66, 6585 ZH, Mook, The Netherlands. m.vercammen@mook.peutz.nl

Summary
Focussing arising from reflections at concave surfaces is a well-known problem in room acoustics. Focussing can cause high sound pressure levels, colouration or an echo. Although the problem is known, the amplification in the focal point and the sound field around the focal point are not. This paper provides some mathematical formulations for sound reflections from concave spherical surfaces. The formulation is based on a wave extrapolation method. The approximations given can be used to calculate the sound field in and around the focal point. The calculation method is verified with an experiment. In the focal point the pressure depends on the wavelength. The width of the peak pressure is also related to the wavelength. For small wavelengths the amplification is high but the area is small, while for lower frequencies the amplification is less, but the area is larger. In a second part of this paper [1] geometrical and engineering methods will be discussed for describing the focussing effect.

PACS no. 43.55.Br, 43.55.Ka

1. Introduction

A well-known problem in room acoustics is the focussing effect arising from concave surfaces. This focussing may be audible through colouration and/or echo effects. Although the phenomenon is well-known, quantification of the problem is not. The purpose of this paper is to investigate the sound reflection from spherically-curved surfaces.

This paper comprises two parts. This first will provide a wave field solution for the sound reflection from a spherical disk. The second will deal with geometrical methods to describe the sound field from an engineering approach, based mainly on the results of this first part.

2. Previous research

One of the most common prediction methods in room acoustics is the geometric approach. Part II of this paper summarises prediction of the sound field by geometrical acoustics for concave surfaces. The essential deficiency of this method is the infinite pressure in the focal point. Nevertheless the geometrical method might enable sufficient prediction for room acoustical purposes (depending on the accuracy one wants to obtain), as long it is only applied at a sufficient distance from the focal point. The sound pressure in the focal point can only be calculated by incorporating the wave character into the calculation method. The Huygens principle can be used for this purpose. In his book on the theory of sound Rayleigh points out [2, §285] that the Huygens principle may also be used for the reflections of sound from curved surfaces, but it is not investigated further mathematically.

A similar situation on the reflection of sound can be found in ultrasonics, where focussed radiators are used. The sound fields generated by these radiators are studied extensively (see e.g.[3, 4, 5]). The phase at the radiator surface is uniform, corresponding to the reflection of sound from a source in the centre of a sphere segment. However the radiators used have a small aperture angle.

A theoretical wave description of the sound field by a parabolic reflector used as a directional microphone is given in [6].

In [7] and [8] the reflected sound field inside cylinders is presented.

In this paper the theory will be applied to room acoustical applications, by extending the theory of 3D radiators to larger aperture angles and for sound sources outside the centre of the sphere. Some validation measurements are presented. A second paper presents an engineering approach to this problem. Parts of this work are presented in [9].

3. Wave-based methods

The Huygens Principle states that every point on the primary wavefront can be thought of as an emitter of secondary wavelets. The secondary wavelets combine to produce a new wavefront in the direction of propagation. From Green's theorem and the Helmholz equation, Kirchhoff formulated the following expression for the sound pressure p at point A in a volume V that is bounded by

Received 18 March 2009,
accepted 20 October 2009.

a surface S (for a sine signal with angular frequency ω):

$$p(A,\omega) = \frac{1}{4\pi}\int_S \left(p(B,\omega)\frac{1+\mathrm{j}kr}{r}\cos\varphi\frac{\mathrm{e}^{-\mathrm{j}kr}}{r} + \mathrm{j}\omega\rho v_n(B,\omega)\frac{\mathrm{e}^{-\mathrm{j}kr}}{r}\right)\mathrm{d}S. \quad (1)$$

The notation is illustrated in Figure 1.

Pressure contributions are calculated from (known) monopole sources and dipole sources. The monopole and dipole source can be calculated from the field radiated from a monopole at distance s from the surface points B:

$$p(B,\omega) = \hat{p}\frac{\mathrm{e}^{-\mathrm{j}ks}}{s}$$

and $$v(B,\omega) = -\frac{1}{\mathrm{j}\omega\rho}\frac{\partial p}{\partial s} = \frac{1}{\rho c}\frac{1+\mathrm{j}ks}{\mathrm{j}ks}\hat{p}\frac{\mathrm{e}^{-\mathrm{j}ks}}{s},$$

and the normal velocity $v_n(\boldsymbol{r},\omega) = \cos\alpha\cdot\boldsymbol{v}(\boldsymbol{r},\omega)$, where $\hat{p}$ is an amplitude factor, chosen so that it yields the pressure at 1 m from the source. So this gives us

$$p(A,\omega) = \frac{\hat{p}}{4\pi}\int_S \left(\frac{1+\mathrm{j}kr}{r}\cos\varphi + \frac{1+\mathrm{j}ks}{s}\cos\alpha\right) \cdot \frac{\mathrm{e}^{-\mathrm{j}k(r+s)}}{rs}\mathrm{d}S. \quad (2)$$

This is a rigorous solution that can be applied not only in the case of a 'virtual' surface S but also for real reflecting boundaries. Theoretically the volume has to be closed, in practice the amplitudes of the secondary sources of parts that do not reflect sound are set to zero. It is noted however that only the first reflection is modelled. Second-order reflections (from the reflector to another part of the reflector and than to point A) are not modelled. These second-order reflections are expected to produce a low noise level, low compared to the pressure in the focal point.

To derive analytic functions from (2) it might be necessary to approximate this function. In the far field ($kr \gg 1$ and $ks \gg 1$) the Fresnel-Kirchhoff diffraction formula is obtained,

$$p(A,\omega) = \frac{\mathrm{j}\hat{p}}{\lambda}\int_S \frac{\cos\varphi+\cos\alpha}{2}\frac{\mathrm{e}^{-\mathrm{j}k(r+s)}}{rs}\mathrm{d}S. \quad (3)$$

In many publications the inclination or obliquity factor $(\cos\varphi+\cos\alpha)/2$ is set to 1; this will further simplify (3) and is correct for large virtual-plane surfaces (Rayleigh integral). For curved surfaces (2) or (3) need to be applied.

4. Integral formulation for a sphere

The geometry of a hemisphere reflector is shown in Figure 2. Using polar co-ordinates, with positions on the sphere described by $z = R\cos\theta$, $x = R\sin\theta\cos\varphi$ and $y = R\sin\theta\sin\varphi$, a small surface element can be described by $\mathrm{d}S = R^2\sin\theta\,\mathrm{d}\theta\,\mathrm{d}\varphi$ and the integral formulation for

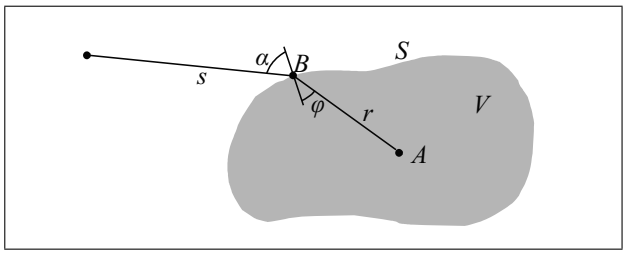

Figure 1. Notation symbols used.

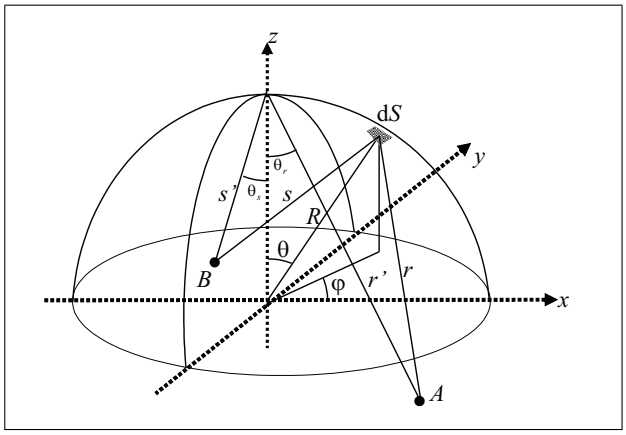

Figure 2. Coordinates used for the sphere.

the pressure of a reflection from this surface becomes

$$p(A,\omega) = \frac{\hat{p}R^2}{4\pi}\int_{\theta=0}^{\pi/2}\int_{\varphi=0}^{2\pi}\sin\theta\left(\frac{1+\mathrm{j}kr}{r}\cos\varphi + \frac{1+\mathrm{j}ks}{s}\cos\alpha\right)\frac{\mathrm{e}^{-\mathrm{j}k(r+s)}}{rs}\mathrm{d}\theta\,\mathrm{d}\varphi. \quad (4)$$

In the case of sphere segments (e.g. a circular sphere segment with $0 \le \theta \le \theta_m$, where θ_m is the opening angle) the integration limits have to be adapted accordingly. Figure 3 shows the result of some numeric calculations with (4) at the $y = 0$ plane (a vertical section of the hemisphere shown in Figure 2).

Note that for high frequencies (e.g. b: $\theta_m = \pi/5$ at 1000 Hz) an illuminated region is obtained with strong interferences, while for low frequencies and low aperture angles a diffusing sound field is obtained (e.g. for f: $\theta_m = \pi/10$ at 250 Hz).

5. Pressure in the focal point

Should the source be positioned in the centre of the sphere, the focal point will be at the same point. At that point $s = r = R$, $\cos\alpha = \cos\varphi = 1$. Assuming $kR \gg 1$ the pressure in the focal point of a hemisphere reduces to

$$p(0,\omega) = \frac{\mathrm{j}\hat{p}}{\lambda}\int_{\theta=0}^{\pi/2}\int_{\varphi=0}^{2\pi}\sin\theta\mathrm{e}^{-\mathrm{j}k2R}\,\mathrm{d}\varphi\,\mathrm{d}\theta = \mathrm{j}k\hat{p}\mathrm{e}^{-\mathrm{j}k2R}. \quad (5)$$

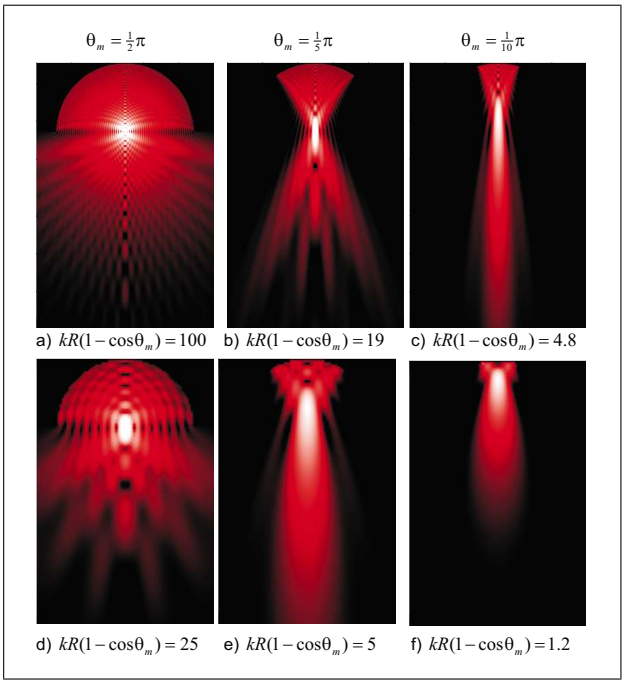

Figure 3. Numeric calculations of the reflected sound field based on (4). For 3 different sizes of the sphere segment ($\theta_m = \pi/2, \pi/5, \pi/10$) and 2 frequencies. The radius R of the sphere segment is 5.4 m. The source is in the centre point. The difference between white and black is 30 dB. Upper row: $f = 1000$ Hz, $k = 18.4$, $kR = 100$, lower row: $f = 250$ Hz, $k = 4.6$, $kR = 25$.

For sphere segments with an opening angle θ_m (for the hemisphere $\theta_m = \pi/2$) the pressure will be $p(0,\omega) = \mathrm{j}k\hat{p}(1-\cos\theta_m)\mathrm{e}^{-\mathrm{j}k2R}$.

The amplitude of the pressure will be

$$\left|p(0,\omega)\right| = k\hat{p}(1-\cos\theta_m). \tag{6}$$

The rms value will be $p^2_{\mathrm{rms}} = {}^1\!/_2\hat{p}^2k^2(1-\cos\theta_m)^2$.

With these results the maximum sound pressure at the focal point, due to reflections against spherically curved surfaces, can be calculated. The result strongly depends on the frequency. High frequencies give very strong amplification at the focal point. It should however be noted that a perfect spherically-curved surface and full reflection is assumed.

The situation with the source in the centre is similar to focussing radiators used for ultrasound. The solution derived by [5] (after translating it to our notation) is $p(0,\omega) = {}^1\!/_2\hat{p}\sin^2\theta_m$. For small aperture angles the factor involving the aperture angles is $(1-\cos\omega_m) \approx {}^1\!/_2\sin^2\theta_m$.

For the description of the sound field the pressure at a certain point A will be related to the pressure at the focal point

$$f(A) = \frac{p(A,\omega)}{p(0,\omega)} = \frac{p(A,\omega)}{\hat{p}k(1-\omega_m)}. \tag{7}$$

6. Approximate solution of the integral

Since there is no primitive function for (4), a closed-form solution of the integral is not possible. With some approximations however a fairly accurate description of the sound field can be obtained, especially for the highest sound pressures.

The co-ordinates for the source B are (x_B, y_B, z_B) and for the receiver A (x_A, y_A, z_A). The distance from the source to the surface element dS is described by

$$\begin{aligned} s^2 &= (R\sin\theta\cos\varphi - x_B)^2 + (R\sin\theta\sin\varphi - y_B)^2 \\ &\quad + (R\cos\theta - z_B)^2 \\ &= R^2 - 2R\sin\theta(x_B\cos\varphi + y_B\sin\varphi) \\ &\quad - 2z_BR\cos\theta + y_B^2 + x_B^2 + z_B^2. \end{aligned}$$

The best possible approximation of the distance, independent of φ or θ, will be the distance from B to the centre of the sphere segment s',

$$\begin{aligned} s'^2 &= (R - z_B)^2 + x_B^2 + y_B^2 \\ &= R^2 - 2z_BR + z_B^2 + x_B^2 + y_B^2, \end{aligned}$$

this will result in

$$\begin{aligned} s^2 &= s'^2 - 2R\sin\theta(x_B\cos\varphi + y_B\sin\varphi) \\ &\quad + 2z_BR(1-\cos\theta). \end{aligned}$$

In the same way the distance from dS to the receiver in A can be determined,

$$\begin{aligned} r^2 &= r'^2 - 2R\sin\theta(x_A\cos\varphi + y_A\sin\varphi) \\ &\quad + 2z_AR(1-\cos\theta). \end{aligned}$$

The first approximation to make is taking the first two terms of the Taylor series.
For $R_A < {}^1\!/_2\sqrt{\lambda R}$ (with R_A: distance from A to the centre):

$$r \approx r' - \frac{R}{r'}\sin\theta(x_A\cos\varphi + y_A\sin\varphi) + \frac{R}{r'}z_A(1-\cos\theta)$$

and

$$s \approx s' - \frac{R}{s'}\sin\theta(x_B\cos\varphi + y_B\sin\varphi) + \frac{R}{s'}z_B(1-\cos\theta).$$

The second approximation, using (4), is only to consider the far field and to assume $\cos\alpha = \cos\varphi = 1$,

$$p(A,\omega) = \mathrm{j}\frac{\hat{p}kR^2}{2\pi}\int_{\theta=0}^{\theta_m}\int_{\varphi=0}^{2\pi}\sin\theta\frac{\mathrm{e}^{-\mathrm{j}k(r+s)}}{rs}\,\mathrm{d}\theta\,\mathrm{d}\varphi, \tag{8}$$

where θ_m is the aperture angle of the sphere segment. Filling in the obtained approximations for r and s (for the amplitude use r' and s')

$$\begin{aligned} p(A,\omega) &= \mathrm{j}\frac{\hat{p}kR^2\mathrm{e}^{-\mathrm{j}k(r'+s')}}{2\pi r's'}\int_{\theta=0}^{\theta_m}\sin\theta\;\mathrm{e}^{-\mathrm{j}kR\left(\frac{z_A}{r'}+\frac{z_B}{s'}\right)(1-\cos\theta)} \\ &\quad\cdot\int_{\varphi=0}^{2\pi}\mathrm{e}^{\mathrm{j}kR\sin\theta\left(\left(\frac{x_A}{r'}+\frac{x_B}{s'}\right)\cos\varphi+\left(\frac{y_A}{r'}+\frac{y_B}{s'}\right)\sin\varphi\right)}\,\mathrm{d}\theta\,\mathrm{d}\varphi. \end{aligned}$$

Using

$$\frac{1}{2\pi}\int\mathrm{e}^{\mathrm{j}z(a\cos\varphi+b\sin\varphi)}\,\mathrm{d}\varphi = J_0\left(z\sqrt{a^2+b^2}\right),$$

where J_0 is the 0-th order Bessel function of the first kind, results in

$$p(A,\omega) = \mathrm{j}\frac{\hat{p}kR^2\mathrm{e}^{-\mathrm{j}k(r'+s')}}{r's'}\int_{\theta=0}^{\theta_m}\sin\theta\mathrm{e}^{-\mathrm{j}kR\left(\frac{z_A}{r'}+\frac{z_B}{s'}\right)(1-\cos\theta)} \cdot J_0\left(kR\sin\theta\sqrt{\left(\frac{x_A}{r'}+\frac{x_B}{s'}\right)^2+\left(\frac{y_A}{r'}+\frac{y_B}{s'}\right)^2}\right)\mathrm{d}\theta.$$

For solving this integral the method used by [5] will be followed: Substituting $u = \sin\theta/\sin\theta_m$ and $\mathrm{d}u/\mathrm{d}\theta = \cos\theta/\sin\theta_m$,

$$p(A,\omega) = \mathrm{j}\frac{\hat{p}kR^2\mathrm{e}^{-\mathrm{j}k(r'+s')}}{r's'} \cdot\int_{u=0}^{1}\frac{\sin^2\theta_m u}{\cos\theta}\mathrm{e}^{-\mathrm{j}k\sin^2\theta_m R/2\left(\frac{z_A}{r'}+\frac{z_B}{s'}\right)u^2} \cdot J_0\left(kR\sin\theta_m u\sqrt{\left(\frac{x_A}{r'}+\frac{x_B}{s'}\right)^2+\left(\frac{y_A}{r'}+\frac{y_B}{s'}\right)^2}\right)\mathrm{d}u.$$

For small θ this can be simplified to

$$p(A,\omega) = \mathrm{j}\frac{\hat{p}R\mathrm{e}^{-\mathrm{j}k(r'+s')}}{s'z_A+r'z_B}Y\int_{u=0}^{1}u\mathrm{e}^{-\mathrm{j}\frac{Y}{2}u^2}J_0\big(Zu\big)\,\mathrm{d}u = \mathrm{j}\frac{\hat{p}R\mathrm{e}^{-\mathrm{j}k(r'+s')}}{s'z_A+r'z_B}I(Y,Z), \tag{9}$$

with

$$Y = kR\sin^2\theta_m(z_A/r'+z_B/s'),$$
$$Z = kR\sin\theta_m\sqrt{(x_A/r'+x_B/s')^2+(y_A/r'+y_B/s')^2},$$
$$I(Y,Z) = Y\int_{u=0}^{1}u\mathrm{e}^{-\mathrm{j}\frac{Y}{2}u^2}J_0(Zu)\,\mathrm{d}u.$$

The latter can be solved by the following power series solution (Lommel integrals):

$$I(Y,Z) = \mathrm{e}^{-\mathrm{j}Y/2}\big(u_1(Y,Z)+\mathrm{j}u_2(Y,Z)\big) \tag{10}$$

with

$$u_1(Y,Z) = \sum_{n=0}^{\infty}(-1)^n\left(\frac{Y}{Z}\right)^{2n+1}J_{2n+1}(Z),$$
$$u_2(Y,Z) = \sum_{n=0}^{\infty}(-1)^n\left(\frac{Y}{Z}\right)^{2n+2}J_{2n+2}(Z).$$

These series will converge for $Y < Z$; this will be in the shadow zone. In the illuminated zone (where $Z < Y$) a better convergence is realised by using

$$u_1(Y,Z) = \sin\left(\frac{Y}{2}+\frac{Z^2}{2Y}\right)-v_1(Y,Z), \tag{11}$$
$$u_2(Y,Z) = -\cos\left(\frac{Y}{2}+\frac{Z^2}{2Y}\right)+v_0(Y,Z), \tag{12}$$
$$v_0(Y,Z) = \sum_{n=0}^{\infty}(-1)^n\left(\frac{Z}{Y}\right)^{2n}J_{2n}(Z), \tag{13}$$
$$v_1(Y,Z) = \sum_{n=0}^{\infty}(-1)^n\left(\frac{Z}{Y}\right)^{2n+1}J_{2n+1}(Z). \tag{14}$$

For practical applications using the first term of v_0 and v_1 will be sufficient,

$$I(Y,Z) = \mathrm{e}^{-\mathrm{j}Y/2}\left(\sin\left(\frac{Y}{2}+\frac{Z^2}{2Y}\right)-\frac{Z}{Y}J_1(Z)+\mathrm{j}\Big[-\cos\left(\frac{Y}{2}+\frac{Z^2}{2Y}\right)+J_0(Z)\Big]\right), \tag{15}$$

$$\big|I(Y,Z)\big| = \left(\left[J_0(Z)-\cos\left(\frac{Y}{2}+\frac{Z^2}{2Y}\right)\right]^2+\left[\frac{Z}{Y}J_1(Z)-\sin\left(\frac{Y}{2}+\frac{Z^2}{2Y}\right)\right]^2\right)^{1/2},$$
$$\big|p(A,\omega)\big| = \frac{\hat{p}R}{s'z_A+r'z_B}\big|I(Y,Z)\big|, \tag{16}$$
$$f(A) = \frac{R}{k(1-\cos\theta_m)(s'z_A+r'z_B)}\big|I(Y,Z)\big|.$$

Based on (15), the sound field at the focal point, on the focal axis, in the focal plane and in the far field will be described in the following sections.

7. Pressure in the focal point based on approximation

7.1. Source in the centre

At the focal point, with the source in the centre, $Y = 0$ and $Z = 0$. Due to the singularity the pressure cannot be calculated with (10) and (16) in the centre, and (9) will be used,

$$p(A,\omega) = \mathrm{j}\frac{\hat{p}kR^2\sin^2\theta_m\mathrm{e}^{-\mathrm{j}k2R}}{R^2}\int_{u=0}^{1}uJ_0\big(0\big)\,\mathrm{d}u = \mathrm{j}\hat{p}k\frac{\sin^2\theta_m}{2}\mathrm{e}^{-\mathrm{j}2kR}. \tag{17}$$

As shown before, $1/2\sin^2\theta_m \approx (1-\cos\theta_m)$ for small θ_m, this yields the same as (6).

7.2. Source position outside the centre

From the definition of Y and Z it can directly be seen that they will be zero (and the focussing effect will be maximum) when $x_A/r' = -x_B/s'$, $y_B/s' = -y_A/r'$ and $z_A/r' = -z_B/s'$.

These relations correspond to the thin lens formula.

However it has to be realised that some approximations are made. In the integration the $\cos\alpha$ and $\cos\varphi$ (see formula 4) should be considered. For $z_A = z_B = 0$ the effect of incorporating this factor in the integration can be approximated by $\approx 1-(x_B^2+y_B^2)/2R^2$. When taking a closer look into the distances r and s one has to realise that changing the angle does influence the distances due to spherical aberration. The effect can be estimated by taking

into account some additional terms of the Taylor series

$$s \approx R - x_B \sin\theta\cos\varphi + \frac{x_B^2}{2R} - \frac{x_B^2 \sin^2\theta\cos^2\varphi}{2R} + \frac{x_B^3 \sin\theta\cos\varphi}{2R^2},$$

$$r \approx R + x_B \sin\theta\cos\varphi + \frac{x_B^2}{2R} - \frac{x_B^2 \sin^2\theta\cos^2\varphi}{2R} - \frac{x_B^3 \sin\theta\cos\varphi}{2R^2},$$

$$r + s \approx 2R + \frac{x_B^2(1 - \sin^2\theta\cos^2\varphi)}{R}.$$

The reduction factor of the pressure at the receiver point can be calculated from

$$f(-x_B) = \frac{1}{2\pi(1-\cos\theta_m)} \cdot \int_0^{2\pi}\int_0^{\theta_m} \sin\theta \mathrm{e}^{-\mathrm{j}k\frac{x_B^2}{R}(1-\sin^2\theta\cos^2\varphi)}\,\mathrm{d}\theta\,\mathrm{d}\varphi$$

using

$$\frac{1}{2\pi}\int_0^{2\pi} \mathrm{e}^{\mathrm{j}z\cos^2\varphi}\,\mathrm{d}\varphi = J_0\big(z/2\big) :$$

$$\frac{\mathrm{e}^{-\mathrm{j}kx_B^2/R}}{2\pi(1-\cos\theta_m)}\int_0^{2\pi}\int_0^{\theta_m} \sin\theta \mathrm{e}^{\mathrm{j}k\frac{x_B^2}{R}(\sin^2\theta\cos^2\varphi)}\,\mathrm{d}\theta\,\mathrm{d}\varphi = \frac{\mathrm{e}^{-\mathrm{j}kx_B^2/R}}{(1-\cos\theta_m)}\int_0^{\theta_m} \sin\theta J_0\Big(k\frac{x_B^2}{2R}\sin^2\theta\Big)\,\mathrm{d}\theta. \qquad (18)$$

A calculation example is given in Figure 4.

It is noted that these effects are not incorporated in the approximate solution in (9). For a source position outside the centre the approximation solution can be seen as a maximum. When the distance of the source to the centre is less than $1/3R$, the error is not more than a factor 2.

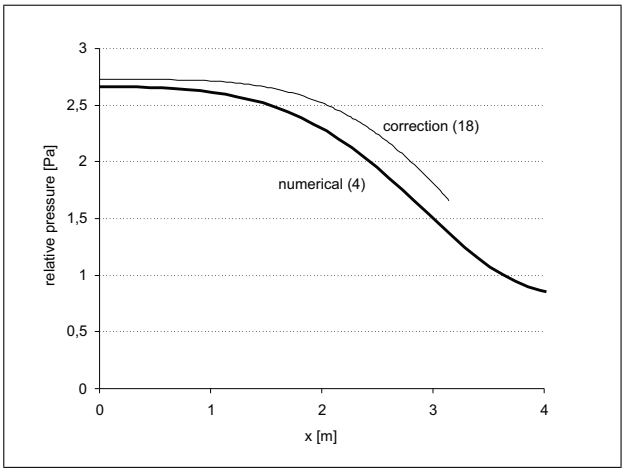

Figure 4. The pressure (relative to $\hat{p}$) at the focal point depends on the distance x of source and receiver from the centre of the sphere. Here for $R = 10\,\mathrm{m}$, $f = 500\,\mathrm{Hz}$, $\theta_m = \pi/4$. Numerical solution with (4) and the approximation with (18) (by numerical integration).

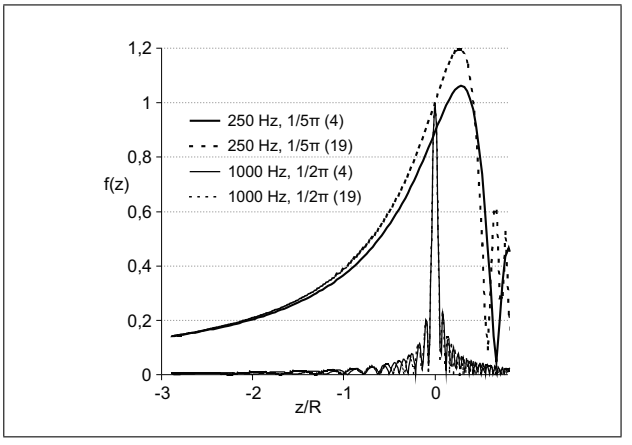

Figure 5. On axis, sound pressure relative to the pressure in the centre. The x-axis is the relative distance z/R to the centre. Results for 1000 and 250 Hz (see Figure 3a and e), obtained by numeric calculation (4) and by (19).

8. Pressure at the axis of the sphere segment

8.1. Source at the centre

First the source will be left in the centre of the sphere while considering the pressure at the receiver position $(0, 0, z_A)$ along the z-axis.

This means that $Y = kR|z_A/(R - z_A)|\sin^2\theta_m$ and $Z = 0$.

Using (16) with $v_0 = 1$ and $v_1 = 0$,

$$\big|I(Y,Z)\big| = \left(\left[1-\cos\left(\frac{Y}{2}\right)\right]^2 + \left[\sin\left(\frac{Y}{2}\right)\right]^2\right)^{1/2} = \sqrt{2}\sqrt{1-\cos\left(kR\left|\frac{z_A}{R-z_A}\right|\frac{\sin^2\theta_m}{2}\right)},$$

$$\big|p(A,\omega)\big| = \frac{\hat{p}R}{s'z_A + r'z_B}\big|I(Y,Z)\big| = \frac{2\hat{p}}{z_A}\sin\left(kR\left|\frac{z_A}{R-z_A}\right|\frac{\sin^2\theta_m}{4}\right), \qquad (19)$$

$$\big|f(A,\omega)\big| \approx \left|\frac{R}{R-z_A}\right| \cdot \frac{\sin\left({}^1\!/_2 kR(1-\cos\theta_m)\left|z_A/(R-z_A)\right|\right)}{{}^1\!/_2 kR(1-\cos\theta_m)\left|z_A/(R-z_A)\right|}.$$

In the centre of the sphere $z_A = 0$, $|f(A,\omega)| = 1$.

Figure 5 shows a comparison between numerical results (4) and (19) for small and large $kR(1-\cos\theta_m)$ (situation from Figure 3a and e). The approximation by (19) gives a slightly higher result but the general result is quite good. It should be noted that in the numeric integration the $\cos\varphi$ (see equation 4) is incorporated; it is not in (19). Furthermore it is noted that for the lower frequency, the maximum is not exactly at the focal point. However the deviation is small.

The 'depth' of the focussing effect, described by the −3 dB points will occur at $|f(A,\omega)| = \sqrt{2}/2$. For $z_A \ll R$ this can be approximated by

$$z_A \approx \pm 0.44 \frac{\lambda}{(1-\cos\theta_m)}.$$

For a further analysis of the decrease with distance it is interesting to see when there are no zeros beyond the focal point. This will occur when in (19)

$$kR\left|\frac{z_A}{R-z_A}\right|\frac{(1-\cos\theta_m)}{2} < kR\frac{(1-\cos\theta_m)}{2} < \pi,$$

so when $kR(1-\cos\theta_m) < 2\pi$.

It is noted that $R(1-\cos\theta_m)$ is the 'depth' of the sphere segment. The condition $kR(1-\cos\theta_m) < 2\pi$ means that less then one wavelength fits in this depth.

The following three situations can be distinguished:
A. depth is more than a wavelength,
B. depth is between a quarter and a full wavelength,
C. depth is less than a quarter wavelength.

Situation A (depth is more than a wavelength): Transition to geometrical decrease with distance

For situation A the point will be considered where the curve will cross the curve of the geometric decrease with distance, assuming the centre point as a (mirror) source (beyond that point strong interferences may be found, but these are of minor concern),

$$\left|p(A,\omega)\right| = \frac{2\hat{p}}{z_A}\sin\left(kR\left|\frac{z_A}{R-z_A}\right|\frac{(1-\cos\theta_m)}{2}\right) = \frac{\hat{p}}{z_A}.$$

This will be for

$$kR\frac{(1-\cos\theta_m)}{2}\frac{z_A}{R-z_A} = n\pi \pm \frac{1}{6}\pi$$

with $n = \ldots, -3, -2, -1, 0, 1, 2, 3, \ldots$

Particularly interesting will be $\pm 5\pi/6$.

Since $kR(1-\cos\theta_m)$ is sufficiently large, the intersection points will be at

$$z_A = \pm\frac{5R\lambda}{6R(1-\cos\theta_m)\pm 5\lambda} \approx \pm\frac{R\lambda}{R(1-\cos\theta_m)\pm\lambda}. \quad (20)$$

This is illustrated in Figure 6. Outside these points the average pressure may be approximated by a geometrical method.

Situation C (depth is less than a quarter wavelength): strong diffraction

When the depth of the segment is less than a quarter wavelength, diffraction from the segment will occur, similar to, or even almost equal to, the diffraction from a flat disk. The pressure amplitude will be inversely proportional to the distance from the sphere instead of the distance from the centre of the sphere,

$$\left|p(z)\right| = \hat{p}\frac{kR(1-\cos\theta_m)}{R-z}, \quad (21)$$

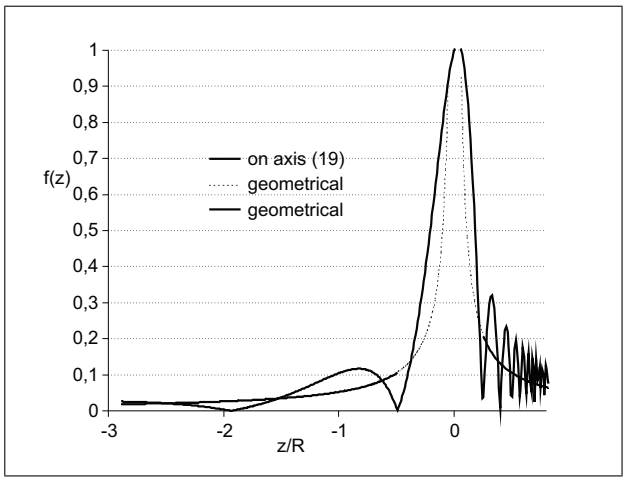

Figure 6. On axis, sound pressure relative to the pressure in the centre for situation A: (depth is more than a wavelength). Shown is the decrease calculated with (19) and the geometrical decrease from the points indicated by (20). Calculation for the situation of Figure 3b: $kR(1-\cos\theta_m) = 19$.

where $R-z$ is the distance from the sphere.

This is valid within 10% for

$$z < \frac{R\sqrt{2.4}}{\sqrt{2.4}+kR(1-\cos\theta_m)}$$

(with $0 < z < R$).

Situation B (depth is between a quarter and a full wavelength)

The situation for $\pi/2 < kR(1-\cos\theta_m) < 2\pi$ can be considered as an 'in between' situation with a virtual monopole somewhere between the sphere segment and the centre. A sort of beam will be obtained, as can be seen in Figure 3 (situation c and e). Formula (19) has to be used to describe the decrease in pressure, also at a larger distance.

8.2. Source position along the axis

For a source out of the centre, but along the axis of the sphere segment $Y = kR\sin^2\theta_m[z_A/(R-z_A) + z_B/(R-z_B)]$ and $Z = 0$, this will result in

$$\left|p(A,\omega)\right| = \frac{2\hat{p}}{z_A+z_B-2z_Az_B/R} \cdot \sin\left(\frac{1}{2}kR(1-\cos\theta_m)\left|\frac{z_A}{R-z_A}+\frac{z_B}{R-z_B}\right|\right). \quad (22)$$

It has to be realised that due to spherical aberration the pressure in the focal point for eccentric situations may be somewhat lower, as explained in section 7.

9. Pressure in the focal plane

9.1. Source at the centre

For calculating the pressure in the focal plane, the source will be placed in the centre of the sphere and the pressure

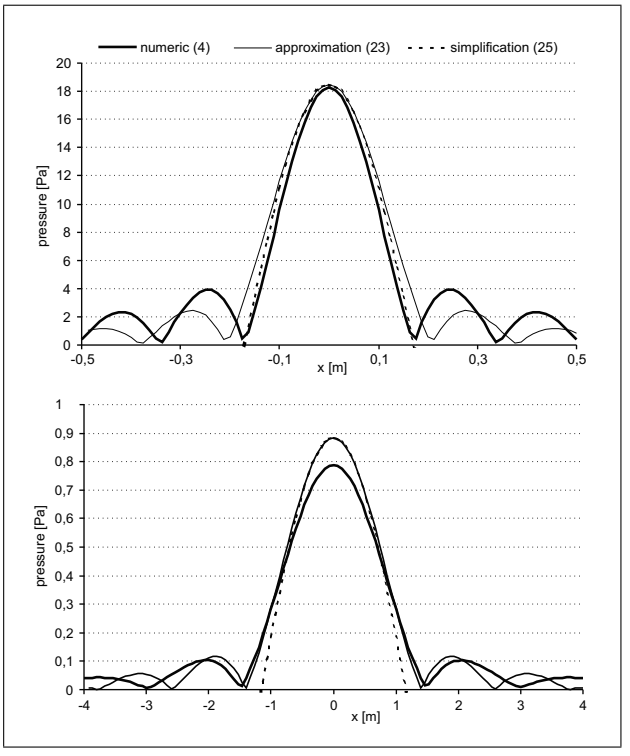

Figure 7. Pressure in focal plane (with $\hat{p} = 1\,\mathrm{N/m}$, radius $R = 5.4\,\mathrm{m}$). Top: 1000 Hz, $\theta_m = \pi/2$ (Figure 3a), bottom: 250 Hz, $\theta_m = \pi/5$ (Figure 3e). Calculated with (4), (23) and (25).

is considered at positions $(x_A, y_A, 0)$. Since this situation is cylindrically symmetrical, $y_A = 0$. For that situation

$$Y = kR\sin^2\theta_m\left(\frac{z_A}{r'} + \frac{z_B}{s'}\right) = 0,$$
$$Z = kR\sin\theta_m \sin\frac{x_A}{r'}.$$

Application of formula (10), with $\lim(Y \to 0)$, only the first term of u_1 is needed, $u_1(0, Z) = J_1(Z)\,Y/Z$ and $u_2 = 0$, so

$$I(Y, Z) = \mathrm{e}^{-\mathrm{j}Y/2}\frac{Y}{Z}J_1(Z),$$

$$\begin{aligned}\left|p(A,\omega)\right| &= \frac{\hat{p}R}{s'z_A + r'z_B}\left|I(Y,Z)\right| \\ &= \hat{p}k\frac{R}{r'}\sin^2\theta_m\frac{J_1\left(kR\sin\theta_m\frac{x_A}{r'}\right)}{kR\sin\theta_m\frac{x_A}{r'}}, \qquad (23)\\ \left|f_{fp}(x_A)\right| &= \frac{p(A,\omega)}{\hat{p}k(1-\cos\theta_m)} \\ &= \frac{R}{r'}\frac{2J_1\left(kR\sin\theta_m\frac{x_A}{r'}\right)}{kR\sin\theta_m\frac{x_A}{r'}}. \qquad (24)\end{aligned}$$

A comparison of (23) with numeric results from (4) is presented in Figure 7.

For $kx_A\sin\theta_m < 2$ ($x_A < \lambda/(\pi\sin\theta_m)$) the function f_{fp} can be simplified by

$$\left|f_{fp}(x_A)\right| \approx \cos\left(\frac{1}{2}kR\sin\theta_m\frac{x_A}{r'}\right). \qquad (25)$$

This will only approximate the main lobe, as can be seen in Figure 7, but that will be sufficient for most purposes in room acoustics.

The width of the lobe, defined by the −3 dB points, will be $-\pi/4 < {}^1\!/_2 kR\sin\theta_m\, x_A/r' < \pi/4$, which is approximately $-\lambda/(4\sin\theta_m) < x_A < \lambda/(4\sin\theta_m)$.

For a hemisphere ($\theta_m = \pi/2$) the total width of the lobe will be $\lambda/2$.

This means the energy will distribute over a certain area, related to the wavelength. The pressure will therefore also be limited and related to wavelength. In the geometrical method the area of the focussing point will be infinitely small, and therefore the pressure infinitely high.

9.2. Source outside the centre

When moving the source along the x-axis: $Y = 0$.

When both source and receiver are on the x-axis ($y_A = y_B = 0$): $Z = kR\sin\theta_m(x_A/r' + x_B/s')$,

$$\begin{aligned}\left|p(A,\omega)\right| &= \frac{\hat{p}R|\mathrm{e}^{-\mathrm{j}Y/2}|}{s'z_A + r'z_B}\left|\frac{Y}{Z}J_1(Z)\right| \\ &= \frac{\hat{p}R}{s'z_A + r'z_B}\left|\frac{kR\sin^2\theta_m\left(\frac{z_A}{r'} + \frac{z_B}{s'}\right)}{kR\sin\theta_m\left(\frac{x_A}{r'} + \frac{x_B}{s'}\right)}\right. \\ &\qquad \left.\cdot\, J_1\left[kR\sin\theta_m\left(\frac{x_A}{r'} + \frac{x_B}{s'}\right)\right]\right|, \\ \left|f_{fp}(x)\right| &= \frac{R^2}{s'r'}\left|\frac{2J_1\left(kR\sin\theta_m\left(\frac{x_A}{r'} + \frac{x_B}{s'}\right)\right)}{kR\sin\theta_m\left(\frac{x_A}{r'} + \frac{x_B}{s'}\right)}\right|. \qquad (26)\end{aligned}$$

For the main lobe $k(x_A + x_B)\sin\theta_m < 2$, so $(x_A + x_B) < \lambda/(\pi\sin\theta_m)$, the function f_{fp} can be simplified by

$$\left|f_{fp}(x_A)\right| \approx \cos\left(\frac{1}{2}kR\sin\theta_m\left(\frac{x_A}{r'} + \frac{x_B}{s'}\right)\right). \qquad (27)$$

This means (approximately) that the pressure field will 'move' to the specular direction.

10. Pressure in the far field

10.1. Source at the centre

The source will be placed in the centre of the sphere again and the pressure in the far field will be considered. This situation is cylindrically symmetrical, so $y_A = 0$ can be assumed, and $x_A/r' = \sin\theta_r$. Since $z_A \gg R$ it can be assumed that $4z_A/r' \approx (z_A - R)/r' = \cos\theta_r$, resulting in

$$\begin{aligned}Y &= kR\sin^2\theta_m\left(\frac{z_A}{r'} + \frac{z_B}{s'}\right) \approx kR\sin^2\theta_m\cos\theta_r, \\ Z &= kR\sin\theta_m\sqrt{\left(\frac{x_A}{r'} + \frac{x_B}{s'}\right)^2 + \left(\frac{y_A}{r'} + \frac{y_B}{s'}\right)^2} \\ &= kR\sin\theta_m\sin\theta_r.\end{aligned}$$

So $Y/Z = \sin\theta_m/\tan\theta_r$ and
$Y/2 + Z^2/2Y = {}^1\!/_2 kR(\sin^2\theta_m\cos\theta_r + \sin^2\theta_r/\cos\theta_r)$.

Should the pressure *near the axis of the sphere segment* ($Z \ll Y$) be considered, it can be assumed that $\cos\theta_r \approx 1$, which results in $Y/2 + Z^2/2Y \approx {}^1\!/_2 kR(\sin^2\theta_m + \sin^2\theta_r)$.

In the illuminated zone, for $Z < Y$, so $\tan\theta_r < \sin\theta_m$, (15) can be used, giving

$$\begin{aligned}\left|I(Y,Z)\right| = \Bigg\{ &\Big[J_0\big(kR\sin\theta_m\sin\theta_r\big) \\ &- \cos\Big(\frac{1}{2}kR(\sin^2\theta_m+\sin^2\theta_r)\Big)\Big]^2 \\ &+ \Big[\frac{\tan\theta_r}{\tan\theta_m}J_1\big(kR\sin\theta_m\sin\theta_r\big) \\ &- \sin\big(\frac{1}{2}kR(\sin^2\theta_m+\sin^2\theta_r)\big)\Big]^2\Bigg\}^{1/2}.\end{aligned} \tag{28}$$

This is only sufficiently accurate for small θ_m and small θ_r.

$$\left|p(A,\omega)\right| = \frac{\hat{p}R}{s'z_A + r'z_B}\left|I(Y,Z)\right|,$$

with the source in the centre:

$$\left|p(A,\omega)\right| = \frac{\hat{p}}{z_A}\left|I(Y,Z)\right|. \tag{29}$$

Formulae (28) and (29) describe the interference pattern in the far field. However the deviations around the geometrical value are limited, so for most room acoustical purposes the geometrical approximation will be sufficient.

There are however some interesting cases to consider: Should $kR(1-\cos\theta_m) = \pi, 3\pi, \ldots, n\pi$ with n be an uneven whole number (the 'depth' of the sphere segment corresponds to $n\lambda/2$), there is a pronounced maximum on the axis ($\theta_r = 0$). For small angles θ_r, $|I(Y,Z)|$ can be approximated by

$$\begin{aligned}\left|I(Y,Z)\right| \approx \Big\{ &1 + J_0\big(kR\sin\theta_m\sin\theta_r\big)^2 \\ &- 2J_0\big(kR\sin\theta_m\sin\theta_r\big) \\ &\cdot\cos\Big(\frac{1}{2}kR(\sin^2\theta_m+\sin^2\theta_r)\Big)\Big]^2\Big\}^{1/2}, \\ \left|I(Y,Z)\right| \approx\ & 1+\cos\Big(\frac{1}{\sqrt{2}}kR(\sin\theta_m\sin\theta_r)\Big).\end{aligned} \tag{30}$$

On the axis ($\theta_r = 0$) this will result in $|I(Y,Z)| = 2$.

The pressure on the axis will be double the pressure based on the geometrical approach.

Formula (30) can be applied for

$$\cos\big(kR\sin\theta_m\sin\theta_r/\sqrt{2}\big) > 0,$$

so

$$\left|kR\sin\theta_m\sin\theta_r/\sqrt{2}\right| < \pi/2,$$

therefore

$$|\sin\theta_r| < \sqrt{2}\lambda/(4R\sin\theta_m).$$

Should $kR(1-\cos\theta_m) = 2\pi, 4\pi, \ldots, n\pi$ with n be an even whole number (the 'depth' of the sphere segment corresponds to $n\lambda/2$), there is a minimum on the axis ($\theta_r = 0$).

Some calculation examples are given in Figure 8.

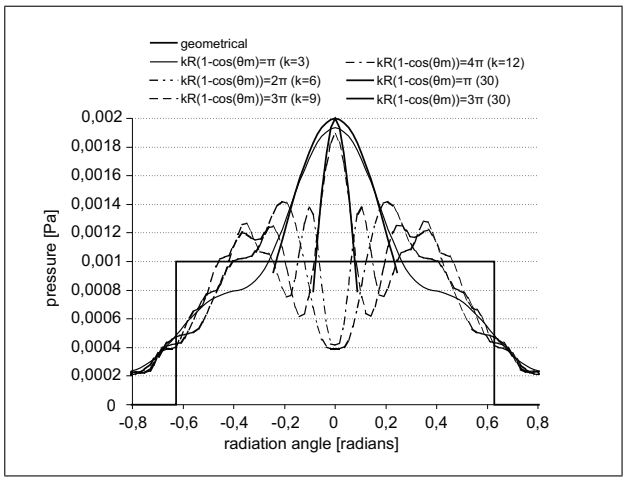

Figure 8. Calculated pressure, using (4), in the far field (1000 m) as a function of the radiation angle. Calculations for different frequencies, corresponding with 'depth' $=n\lambda/2$. $R = 5.4$ m, $\theta_m = \pi/5$. Also showing the approximated peaks using (30).

The pressure at the borders of the illuminated area (in the case of Figure 8 indicated by the geometrical approach: $\pm\theta_m = \pm\pi/5 \approx \pm 0.62$) are roughly half the geometrical pressure.

For small depth of the sphere segments,

$$kR(1-\cos\theta_m) \le \pi/2,$$

a diffusing sound field will be obtained, outside the borders of the 'illuminated' area.

For this small depth the pressure on the axis $\sin\theta_r = 0$ will be

$$\left|p(A,\omega)\right| \approx \frac{\hat{p}}{z_A}kR\sin^2\theta_m.$$

Defining the 'radius' $a = R\sin\theta_m$ and the area $S = \pi a^2$ of the sphere segment,

$$\left|p(A,\omega)\right| = \hat{p}\frac{2S}{\lambda R z_A}.$$

This is equal to the well-known Fraunhofer diffraction. Depending on the radiation angle θ_r the pressure can be approximated with

$$\left|p(A,\omega)\right| = \hat{p}\frac{ka^2}{Rr'}\frac{\sin(ka\sin\theta_r)}{ka\sin\theta_r}. \tag{31}$$

Some calculation examples are given in Figure 9.

10.2. Source outside the centre

Firstly the source will be positioned outside the centre of the sphere on the z-axis ($x_B = y_B = 0$) and the pressure in the far field will be considered.

This will be a symmetrical situation, so $y_A = 0$ can be assumed.

$$Y = kR\sin^2\theta_m\big(\cos\theta_r + z_B/s'\big).$$

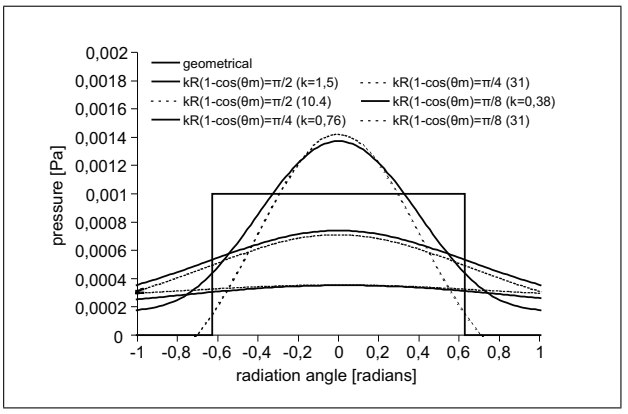

Figure 9. Calculated pressure for small depth, using (4) (solid lines), in the far field (1000 m) as a function of the radiation angle. Calculations for different frequencies, corresponding with 'depth'= $\lambda/4$, $\lambda/8$, $\lambda/16$, $R = 5.4$ m, $\theta_m = \pi/5$. Also showing the approximation (dashed) with Fraunhofer diffraction using (31).

And Z will remain, $Z = kR\sin\theta_m \sin\theta_r$.

$$\frac{Y}{2} + \frac{Z^2}{2Y} = \frac{1}{2}kR\left(\sin^2\theta_m\left(\cos\theta_r + z_B/s' \right) + \frac{\sin^2\theta_r}{\left(\cos\theta_r + z_B/s' \right)} \right).$$

For $x_A = \sin\theta_r = 0$ (on the z-axis): $Z = 0$ and $Y/2 + Z^2/2Y = {}^1\!/_2 kR\sin^2\theta_m(1 + z_B/s')$, so

$$\left| I(Y,Z) \right| = \left\{ \left[J_0(Z) - \cos\left(\frac{Y}{2} + \frac{Z^2}{2Y} \right) \right]^2 + \left[\frac{Z}{Y} J_1(Z) - \sin\left(\frac{Y}{2} + \frac{Z^2}{2Y} \right) \right]^2 \right\}^{1/2}$$

$$\approx \sqrt{2 - 2\cos\left(\frac{1}{2}kR\sin^2\theta_m \left(1 + \frac{z_B}{s'} \right) \right)}$$

$$\left| p(A,\omega) \right| = \frac{\hat{p}R}{s'r'(1 + z_B/s')} \cdot \sqrt{2 - 2\cos\left(\frac{1}{2}kR\sin^2\theta_m \left(1 + \frac{z_B}{s'} \right) \right)}. \quad (32)$$

The first part of (32) describes the geometrical effect, while the root describes the interference (between 0 and 2), similar to the situation with the source in the centre. The maximum will occur at a different 'depth' of the sphere segment.

Secondly the source will be moved along the x-axis ($z_B = y_B = 0$) and the pressure in the far field will be considered.

Assuming $y_A = 0$, and $x_A/r' = \sin\theta_r$ and $x_B/s' = \sin\theta_s$:

$$Y = kR\sin^2\theta_m \cos\theta_r,$$
$$Z = kR\sin\theta_m(\sin\theta_r + \sin\theta_s).$$

At the specular axis, for $\theta_r = -\theta_s$, $Z = 0$ and the result will be similar to that at the z-axis with the source in the centre. The pressure field is rotated over an angle $-\theta_s$.

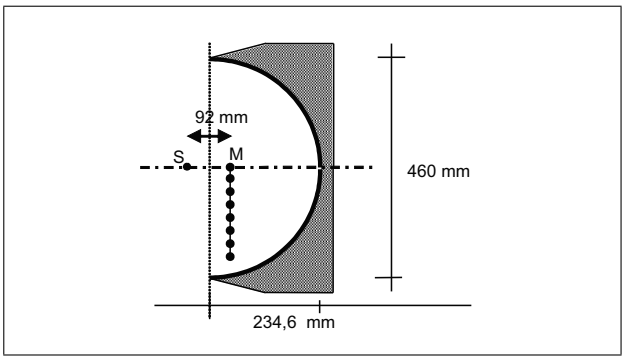

Figure 10. Section of the experimental setup (half ellipsoid), S = source, M = microphone.

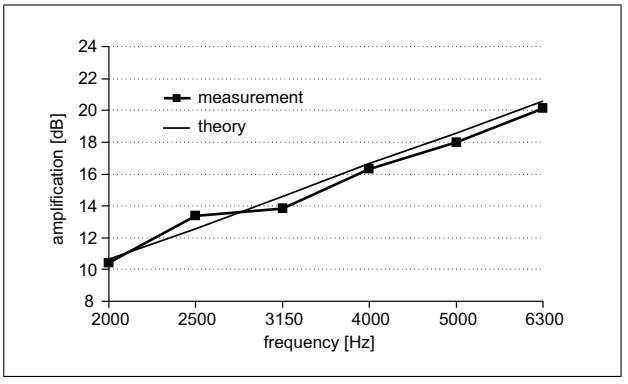

Figure 11. Difference between the sound pressure level of the reflected and the direct sound in the focal point, calculation result (2) and measurement results (both 1/3 oct. values).

11. Experimental verification of the amplification in the focal point

To verify the theoretical amplification at the focal point an experimental set-up was made on a small scale. It consists of half an ellipsoid with the two focal points at a relatively small distance. By using an elliptical shape, the source and microphone can be at different locations. The measurement set-up is shown in Figure 10. The source is in one of the focal points.

The model was milled by CAD/CAM from a solid polyurethane block (Ebaboard PW 920), a material with a high density and excellent low surface porosity. The accuracy of the shape of the ellipsoid is approx. 0.01 mm.

The impulse response was measured with an MLS (Maximum Length Sequence) signal. In the time domain the separation of direct signal and (single) reflected signal was made. The geometry was optimised to obtain sufficient time separation between direct sound and reflection, especially in the focal area.

The sound pressure at the microphone position is also calculated, using (2), by numerical integration of the Kirchhoff integral (2) over the half ellipsoid. The increase of the reflected sound pressure level measured and calculated in respect to the direct sound pressure level is shown in Figure 11. Figure 12 shows the pressure along the focal plane, as indicated in Figure 10. The results show good

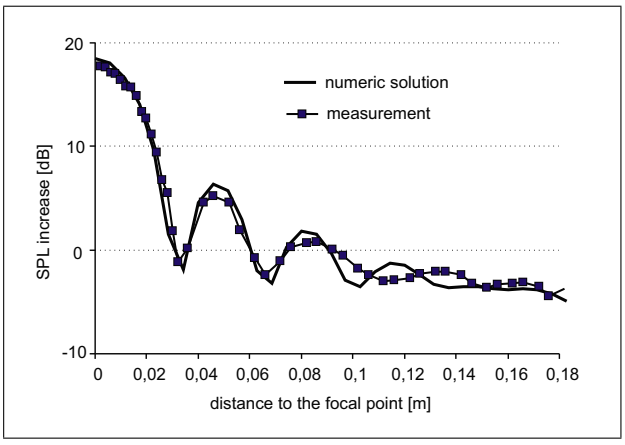

Figure 12. Sound pressure level relative to the direct sound at 5000 Hz (1/3 oct.), along the axis on the focal plane (see Figure 10). Numeric solution (2) and measurement result.

agreement with the theory, confirming the validity of (2). This comparison does not include possible deviations due to the approximation method, as described in sections 7–10.

12. Conclusions

This paper has provided some mathematical formulations for sound reflections from concave spherical surfaces. The formulation is based on a wave extrapolation method. The approximations given can be used to calculate the sound field in and around the focal point.

At the focal point the pressure depends on the wavelength and the opening angle of the sphere segment. It does not depend on the radius of the sphere. The width of the peak pressure is also related to the wavelength. For small wavelengths the amplification is high but the area small, while for lower frequencies the amplification is less, but the area is larger.

The validity of the basic integral describing the reflection from a curved surface is verified with an experiment.

Part II of this paper [1] will discuss a geometrical method and an engineering method will be presented to estimate the sound pressure.

References

[1] M. Vercammen: Sound reflections from concave spherical surfaces. Part II: Geometrical acoustics and engineering approach. Acta Acustica united with Acustica **96** (2010).

[2] J. W. Strutt, Baron Rayleigh: Theory of sound. 1896. Dover Publications, 1945.

[3] H. T. O'Neil: Theory of focussing radiators. J. Acoust. Soc. Am. **21** (1949).

[4] B. G. Lucas, T. G. Muir: The field of a focussing source. J. Acoust. Soc. Am. **72** (1982).

[5] K. Q. S. X. Chen, K. J. Parker: Radiation pattern of a focussed transducer: A numerically convergent solution. J. Acoust. Soc. Am. **94** (1993).

[6] S. Wahlström: The parabolic reflector as an acoustical amplifier. J. Audio Eng. Soc. **33** (1985) 6.

[7] H. Kuttruff: Some remarks on the simulation of sound reflection from curved walls. Acustica **77** (1993) 176.

[8] Y. Yamada, T. Hidaka: Reflection of a spherical wave by acoustically hard, concave cylindrical walls based on the tangential plane approximation. J. Acoust. Soc. Am. **118** (2005).

[9] M. Vercammen: The reflected sound field by curved surfaces. Proc. Acoustics'08, Paris, 2008.